MRS. IWONA SKIBA-KUREK (Orcid ID : 0000-0002-0533-2130)

Article type : Research Article

Design, synthesis and activity against *Staphylococcus epidermidis* of 5-chloro-2- or 5-chloro-4-methyl-9*H*-xanthen-9-one and some of its derivatives

Running title: Antibacterial activity of new xanthone derivatives

Gabriela Mazur [a], Iwona Skiba-Kurek [b], Elżbieta Karczewska [b], Katarzyna Pańczyk-Straszak [a], Joanna Jaworska [a], Anna M. Waszkielewicz [a]*

[a] *Department of Bioorganic Chemistry, Chair of Organic Chemistry, Faculty of Pharmacy, Jagiellonian University Medical College, ul. Medyczna 9, 30-688 Krakow, Poland*

[b] *Department of Pharmaceutical Microbiology, Faculty of Pharmacy, Jagiellonian University Medical College, ul. Medyczna 9, 30-688 Krakow, Poland*

* anna.waszkielewicz@uj.edu.pl, tel. +4812-6205576

Acknowledgements

This work was financed from Jagiellonian University Medical College statutory funds N42/ DBS/000032 and K/ZDS/007776. This article is also a result of the research project No. 2018/31/N/NZ6/03339 financed by the National Science Centre, Poland.

Ten new xanthone derivatives have been designed and synthesized for their potential antibacterial activity. All compounds have been screened against *Staphylococcus epidermidis* strains ATCC

12228 and clinical K/12/8915. The highest antibacterial activity was observed for compound **3**: 5-chloro-2-((4-(2-hydroxyethyl)piperazin-1-yl)methyl)-9*H*-xanthen-9-one dihydrochloride, exhibiting MIC of 0.8 μg/mL against ATCC 12228 strain, compared to linezolid (0.8 μg/mL), ciprofloxacin (0.2 μg/mL) or trimethoprim and sulfamethoxazole (0.8 μg/mL). For the most active compound **3**, genotoxicity assay with use of *Salmonella enterica* serovar *Typhimurium* revealed safety in terms of genotoxicity at concentration 75 μg/mL and antibacterial activity against *Salmonella* at all higher concentrations. A final *in silico* prediction of skin metabolism of compound **3** seems promising, indicating stability of the xanthone moiety in the metabolism process.

Key words: antibacterial, xanthone, synthesis, *Staphylococcus epidermidis, Salmonella enterica, UMU-test*

1. Introduction

Staphylococcus epidermidis is Gram-positive bacteria belonging to coagulase negative staphylococci (CNS) group. It is an important element of the physiological flora, colonizing the skin around the armpits, scalp and nasal atrium (Namvar et al., 2014). *Staphylococcus epidermidis* is also an important opportunistic pathogen causing hospital infections particularly in neonatal intensive care units (NICU) (Eftekhar & Speert, 2009). Blood infections with such pathogens are especially dangerous for newborns whose immune systems are extremely immature and in whom invasive treatments are very frequently applied during hospitalization (Cheung & Otto, 2010; Nash et al., 2013). Rapid and accurate diagnosis of neonatal sepsis is of key importance due to high morbidity and mortality affecting approximately 40% of patients (Zea-Vera & Ochoa, 2015; Fell et al., 2017).

Increasing resistance to antimicrobial agents among *Staphylococcus epidermidis* clinical strains, in particular lack of susceptibility to β-lactam antibiotics or macrolides, lincosamides and streptogramins B is currently a serious therapeutic and epidemiological problem (Bizzarro et al., 2015). A high percentage of *Staphylococcus epidermidis* isolates acquired from neonates are resistant to antibiotics: β-lactams (86% – 100%), erythromycin (65% – 100%) and clindamycin (80% – 100%) (Brzychczy-Włoch et al., 2013). In addition, this species has the ability to produce

biofilm that increases the pathogenicity of *Staphylococcus epidermidis* and resistance to antibacterial drugs used in therapy (Büttner, Mack & Rohde, 2015; Wojtyczka et al., 2014). The biofilm constitutes extracellular polysaccharide which is termed by polysaccharide intercellular adhesin (PIA) in *S. epidermidis* (Fitzpatrick, Humphreys & O'Gara, 2005).

The xanthone moiety (9*H*-xanthen-9-one, dibenzo-γ-pyrone) is a naturally occurring heterocyclic structure, present in medicinal plants such as *Garcinia mangostana* (α-mangostin, Fig. 1) (Jung et al., 2006; Dharmaratne et al., 2013), *Mangifera indica* (Pinto, Sousa & Nascimento, 2005), *Cudrania cochinchinensis* (Fukai et al., 2005), *etc*. Therefore, there have been many attempts to search for biological activity within the group of derivatives of xanthone, where significant biological activities have been found, such as: anticancer (Szkaradek et al., 2016), anticonvulsant (Szkaradek et al., 2013; Waszkielewicz et al., 2013), antioxidant (Jung et al., 2006), antifungal (Klesiewicz et al., 2018), antimicrobial (Fukai et al., 2005), *etc.* – some amount of research has been performed by our team.

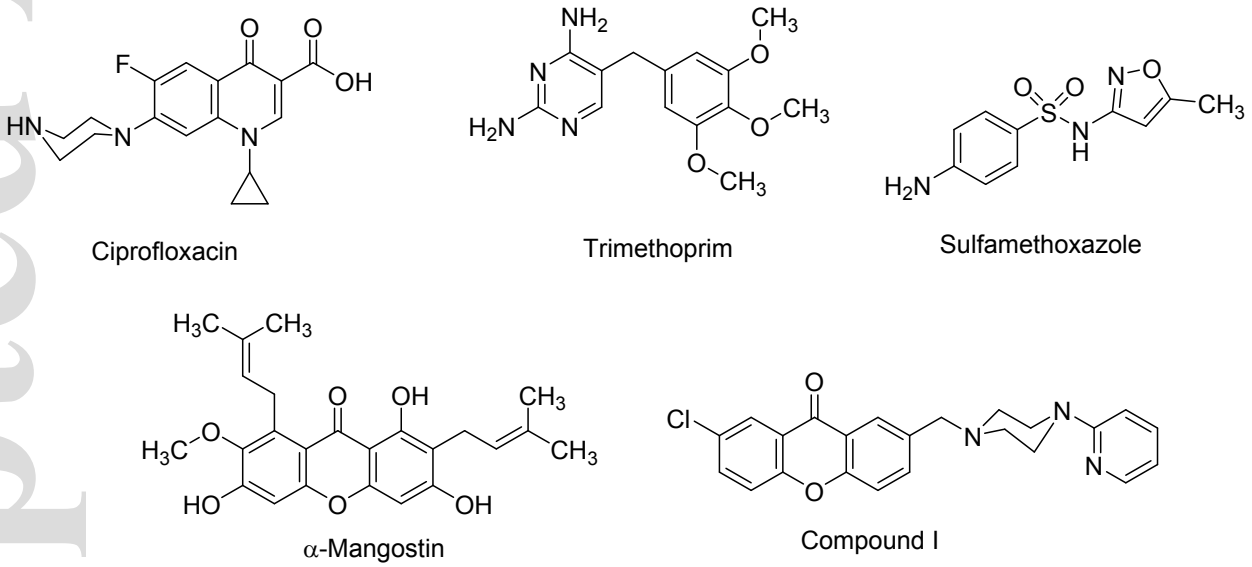

Fig. 1 Popular chemotherapeutics - control and reference compounds: α-mangostin – a natural antibacterial xanthone derivative and synthetic antifungal compound **I** (Klesiewicz et al., 2018).

New synthetic xanthone derivatives as well as other groups of compounds and their antibacterial activity have been already studied by our research team. So far, some significant activity against the bacteria *Helicobacter pylori* have been found (Klesiewicz et al., 2016). We noticed interesting

influence in antibacterial activity of chlorine substituent in xanthone derivatives in positions 6 or 7 as well as in 4-chlorophenoxyalkylamines (Klesiewicz et al., 2018), therefore, the substituent remains interesting for us when attempting drug design for new antibacterial compounds. This time we aimed to try a new position – C5. Moreover, we have noticed significant input of piperazine moiety into antimicrobial activity and this moiety also remains important in our drug discovery work (Klesiewicz et al., 2016).

The purpose of this research is design, synthesis and evaluation of antibacterial activity of some new xanthone derivatives, against *Staphylococcus epidermidis* bacteria. Since the xanthone moiety by itself exhibits antimicrobial activity, we attempted to enhance it with possible additional substituents. The general attempt was to achieve xanthone derivatives with chlorine in position 5, methylene linker in positions 2 or 4, linking with a moiety built of ethylene alkyl groups connected by proton acceptors (O) or proton donors (NH). Such structure was hoped for creating hydrogen bonds with any water or polysaccharides in bacterial biofilm. Such interactions would enable the lipophilic antibacterial chloroxanthone penetrate the biofilm.

2. Results and discussion

2.1. Chemistry

Ten new xanthone derivatives have been designed and synthesized for their potential antibacterial activity, in terms of chlorine and piperazine containing substituents. Chlorine in position C5 has been introduced for enhancement of antibacterial activity due to our former observations. Hydrophilic substituents have been introduced in position C2 or C4, for affinity to the aforementioned polysaccharide biofilm. The first obtained compounds were hydroxyethyl or hydroxyethoxyethyl derivatives of 5-chloro-2- or 5-chloro-4-(piperazinemethyl)xanthone. As our research advanced, we designed pyridine analog, on the basis of formerly beneficial properties of *N*-(2-pyridine)piperazine derivatives in our antimicrobial activity research and due to the structure of reference compound **I** (Fig. 1) (Klesiewicz et al., 2018), as well as two more lipophilic structures. We also synthesized three compounds lacking piperazine ring, in order to evaluate the influence of the presence of piperazine moiety on antibacterial activity. Since we achieved favorable results for lipophilic substituted derivatives which were poorly soluble in water, it was necessary to achieve the compounds in the form of hydrochlorides for the significant issue of affinity towards bacterial biofilm. The form of hydrochloride was possible to achieve in case of 2

amine groups in the piperazine moiety. Additionally, the chemical characteristics of the aforementioned biofilm (also produced by *S. epidermidis* K/12/8915 strain) could require ionized form of the designed compounds for being mixed and absorbed into proximity of the bacterial cell membrane. The obtained structures are presented in Table 1.

Additionally, part of our research is analysis how molecular properties such as lipophilicity, molecular volume, or topological polar surface area (TPSA) influence the biological properties. Especially that these properties can influence cell membrane permeation and further absorption of the compound in the bacteria cell. So far, literature concerning properties of antibacterial compounds against *Staphylococcus aureus* has described logP range varying between -0.75-4.88 (Wadapurkar et al., 2018). Therefore, our findings are interesting in order to plan further research of antibacterial compounds.

Table 1 Structures, calculated physical-chemical data and antibacterial activity of the title compounds **1-10.**

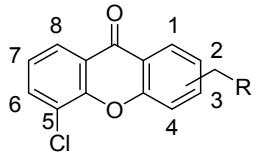

Compound	Position	R	logP [a]	mV [a] ($Å^3$)	TPSA [a] ($Å^2$)	MIC (μg/mL) *Staphylococcus epidermidis*	
						ATCC 12228 strain	K/12/8915 strain
1	**C2**	-H	4.62	202.68	30.21	50	50
2		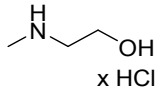 x HCl	3.40	240.14	62.47	50	50
3		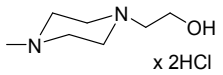 x 2HCl	3.24	326.47	56.91	0.8	50
4		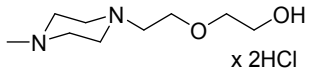 x 2HCl	3.13	369.06	66.15	50	50
5		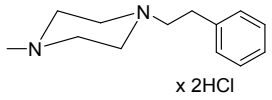 x 2HCl	5.67	389.86	36.69	6.25	50
6		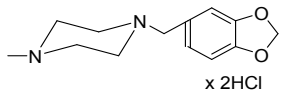 x 2HCl	5.16	396.99	55.16	50	50
7		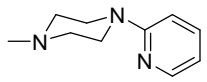 x 3HCl	4.67	352.1	49.58	50	50

8	**C4**	-H	4.60	202.68	30.21	50	50
9		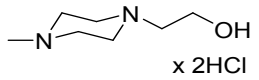 x 2HCl	3.7	227.74	50.44	50	50
10		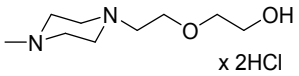 x 2HCl	3.59	270.32	59.67	50	50
Linezolid [b]						0.8	1.6
Ciprofloxacin [b]						0.2	0.4
Trimethoprim/Sulfamethoxazole in a ratio of 1:19 [b]						0.8	1.6

[a] data calculated from www.molinspiration.com; mV – molecular volume; TPSA – topological polar surface area

[b] quality control (*Staphylococcus aureus* ATCC 29213, EUCAST QC Tables): Linezolid MIC = 1.6 μg/mL, Ciprofloxacin MIC = 0.4 μg/mL, Trimethoprim/Sulfamethoxazole in a ratio of 1:19 MIC = 0.4 μg/mL

The title compounds **1**-**10** were synthesized similarly to previously published procedures (Waszkielewicz et al., 2013) and the synthesis is presented in Scheme 1. The first step constituted the Ullmann's condensation resulting in formation of the 5-chloro-2- or 5-chloro-4-methylxanthone skeleton – with use of 2,3-dichlorobenzoic acid and appropriate cresol (*para* for **1**-**7** or *orto* for **8**-**10**). The reaction was performed for a few hours, in paraffin oil, at 180 °C, in the presence of Cu/Cu_2O catalyst. After condensation, intermediate product underwent cyclization in the presence of H_2SO_4 (98%) resulting in 5-chloro-2-methyl-9*H*-xanthen-9-one (Eckstein & Marona, 1980) (for **1**-**7**) or 5-chloro-4-methyl-9*H*-xanthen-9-one (Rewcastle et al., 1989) (for **8**-**10**). For compounds **1** and **8** this step was the final one. For all other compounds free-radical bromination of the methyl residue with *N*-bromosuccinimide (NBS) was performed in CCl_4, in the presence of benzoyl peroxide under UV-light, resulting in 5-chloro-2-bromomethyl-9*H*-xanthen-9-one (Eckstein & Marona, 1980) or 5-chloro-4-bromomethyl-9*H*-xanthen-9-one (Rewcastle et al., 1989), respectively. The final step for compounds **2**-**7**, **9** and **10** was aminolysis of the appropriate bromo-substituted derivative by means of commercially available amines: colamine for **2**, *N*-(hydroxyethyl)piperazine for **3** and **9**, *N*-(2-hydroxyethoxyethyl)piperazine for **4** and **10**, *N*-(phenylethyl)piperazine for **5**, *N*-piperonylpiperazine for **6** and *N*-(2-pyridyl)piperazine for **7**. The reaction was carried out in toluene in the presence of anhydrous K_2CO_3 as a proton acceptor. The obtained amines were washed out from ethanol : water (96 : 4 v/v) mixture. Some portions of products solutions were converted into hydrochlorides using addition of 37% HCl solution in water. The salts were purified by means of recrystallization from methanol. Compounds lacking amine moiety (**1** and **8**) were crystallized from ethanol.

Due to high solubility of compounds required for the antibacterial assays, all achieved bases were converted to hydrochlorides as described above, and evaluated in this form. However, the mass spectrometry allows only to show the mass of the base form, and protons in the salt form were not visible in ^1H NMR (expected broad singlet at chemical shift *ca.* 9-11 ppm) for most compounds. The achievement of the proper salts of the title compounds was confirmed by means of elemental analysis. For compounds **1-4** and **8** additional ^{13}C NMR spectra have been obtained.

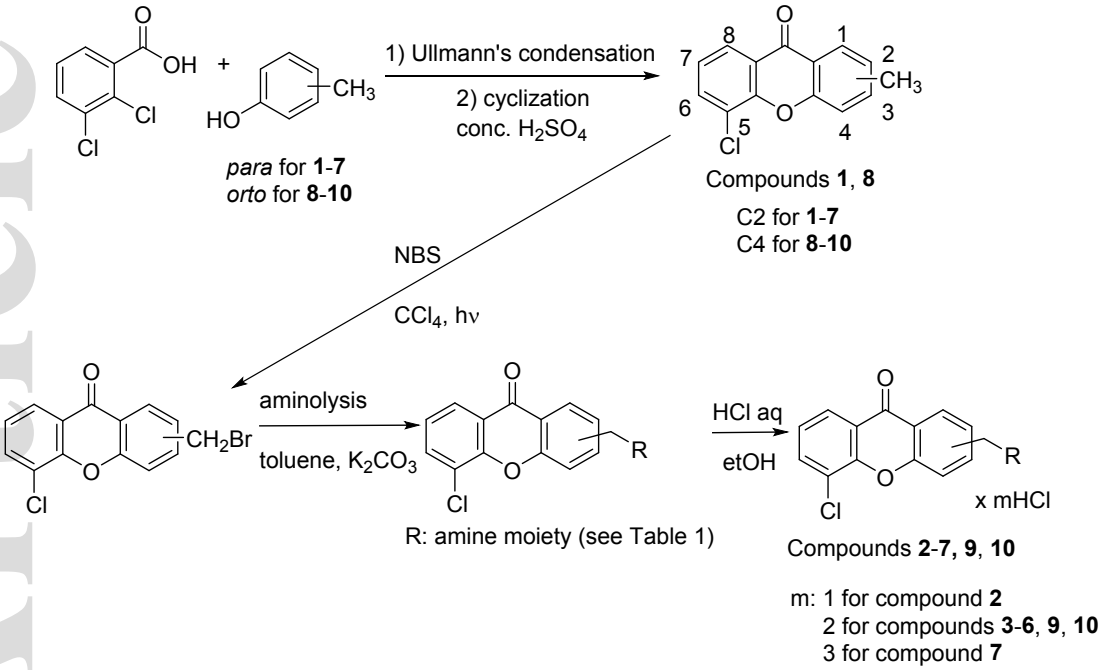

Scheme 1 Synthesis of the title compounds **1**-**10**.

2.2. Microbiology

Compounds **3** and **5** were the most active with MIC values equal to 0.8 and 6.25 μg/mL, respectively – comparable with those obtained for reference chemotherapeutic agents (http://www.Eucast.Org/Ast_of_bacteria/Media_preparation/).

Interesting observations can be made in terms of position isomerism. Within this group of compounds, compound **8** is a positional isomer of compound **1**, compound **9** is a C4 positional isomer of compound **3**, and similarly compound **10** is the C4 isomer of compound **4**. In case of amines (compounds **3**, **4**, **9**, **10**) the molecular volume of the C2 derivatives is larger than that of C4 derivatives – which could be predicted based on position C5 already taken by Cl atom and the shape of the compound. Nevertheless, both two most active compounds **3** and **5** are C2 substituted xanthone derivatives and are more active than *e.g.* compound **9** – C4 analogue of **3**. Therefore, it can be concluded in this small group that the C2 position seems favourable for the antibacterial activity. This is unexpected because position C2 brings larger volume of the compound (Table 1), while smaller compounds are usually expected to be absorbed easier than big ones into the bacteria membrane.

LogP values of the most active compounds **3** and **5** are 3.24 and 5.67, respectively, while the range of logP in this group is 3.13-5.67 – therefore it can be concluded that in this group of compounds lipophilicity is not determinant for their activity, and this is contrary to the assumptions taken at the design of the structures.

Considering our assumptions regarding incorporating proton acceptors or donors in the designed structures for the enhancement of antibacterial activity of xanthone, compounds **1** and **8** lacking amine/hydroxy group were inactive. On the other hand, compound **4** should be more active than **3** – and this assumption did not prove correct. Compound **4** as hydroxyethoxyethylpiperazine derivative can produce more hydrogen bonds than **3** as hydroxyethylpiperazine derivative and this feature did not prove beneficial. The most active are compounds **3** – hydroxyethylpiperazine derivative and compound **5** – phenethylpiperazine derivative. Therefore, incorporation of piperazine moiety for possibility to achieve dihydrochlorides as a common feature of the two compounds, as well as position C2 of the substitution of the 5-chloroxanthone moiety, seem favourable.

The molecular mechanism of antimicrobial activity observed for compounds **3** and **5** remains unclear. However, literature data provide some hypotheses. Within xanthone derivatives exhibiting antimicrobial activity against *S. epidermidis*, α-mangostin is the most studied one. Combination of transcriptome and proteome analyses with a use of *S. epidermidis* RP62A showed that α-mangostin perturbs cytoplasmic membrane by hydrogen bonds formation with transmembrane precursor proteins. This process leads to downregulation of genes important for multiple metabolic pathways (Sivaranjani et al., 2019). Taken the above into account, cytoplasmic membrane is likely to be a principal target for compounds **3** and **5**, especially that both compounds possess hydrogen bond donors and acceptors in their structure both within the xanthonic system and the side chain. This hypothesis needs to be tested experimentally.

The difference of activity of compounds **3** and **5** between the strain *Staphylococcus epidermidis* ATCC 12228 and clinical strain *Staphylococcus epidermidis* K/12/8915 can result from presence of biofilm in K/12/8915 and its absence in the reference ATCC 12228. Moreover, the K/12/8915 is characterized by multidrug resistance. Drug resistance of bacterial strains is a major challenge in the design of new antibiotics and acts as a driving force for this branch of medical chemistry. The drug resistance mechanisms developed by bacteria include the expression of enzymes involved in the degradation of antibiotic molecules, decreased membrane permeability, mutations within

antibiotic molecular targets or efflux pumps activation. Common strategies of antibiotic resistance mitigation target particular drug classes or single strains of resistant microbe (Riduan, Armugam & Zhang, 2020). Modern strategies include among others search for new molecular targets for antibiotics, design of multitarget drugs, consideration of adjuvant therapies disrupting cell membrane and deactivating efflux pumps, as well as utilization of reactive oxygen species in antimicrobial therapy (Riduan, Armugam & Zhang, 2020; Perdih et al., 2015; Perdih et al., 2014; Baym, Stone & Kishony, 2016; Monserrat-Martinez, Gambin & Sierecki, 2019; Dersch et al., 2017; Wright, 2016). Within xanthone derivatives, α-mangostin is known to be active against many drug-resistant strains, probably due to its mechanism of action involving cell membrane perturbation and – as a consequence – influence on multiple metabolic pathways (Sakagami et al., 2005; Koh et al., 2013). The xanthon and α-mangostin derivatives therefore represent a promising group of compounds in the context of combating antibiotic resistance.

Formation of biofilm by bacterial strains constitutes another problem. Insufficient drug penetration through the biofilm may lead to reduced or ineffective therapy (Singh et al., 2010). *S. epidermidis* biofilm formed on medical devices causes a real threat. Literature data suggest potential use of α-mangostin and its derivatives also against biofilm-forming strains of *S. epidermidis* (Sivaranjani et al., 2017). As compounds **3** and **5** turned out to be active against a strain that does not form biofilm, it is not possible to make conclusions regarding their biofilm penetration. Further studies on this issue would be worthy. Due to low MIC values, both compounds are promising for treatment of infections with *S. epidermidis*. There exist premises for further research both in this group of compounds for other strains (including presence and absence of biofilm), as well as in design and synthesis of new antibacterial compounds.

2.3. Genotoxicity

The most active compound **3** was chosen for additional safety testing, for the purpose of elimination of genotoxic compounds at an early stage. UMU-Chromotest (commercially available kit) was used for this purpose. The assay utilizes an engineered *Salmonella enterica* serovar *Typhimurium* strain which possesses a gene coding for the β-galactosidase enzyme tethered to the *umuC* gene (one of damage response genes, a part of SOS genetic material repair system). In case of DNA damage, the SOS system is activated, β-galactosidase gene gets transcribed proportionally to the level of SOS induction and enzyme activity can be detected calorimetrically (Reifferscheid et al., 1991).

The compound was tested in five concentrations ranging 75-1200 µg/mL (Table 2). In order to receive reliable results, the protocol includes calculation of growth factor G (G < 0.5 indicates toxicity of tested sample towards the used bacterial strains and makes the experiment unreliable). Due to low G values, evaluation of genotoxic properties was feasible only at concentration 75 µg/mL, at which the compound proved safe (induction ratio I_R < 1.5). Additionally, the low G values obtained may be a premise for search for antibacterial activity against *Salmonella enterica* serovar *Typhimurium* strain in a group of xanthone derivatives, which is surprising, but very promising observation.

Table 2 Results of UMU test for compound **3**

Compound	Concentration [µg/mL]	G[a]	U_s[b]	I_R[c]
3	75	0.799	0.639	0.800
	150	0.473	NT	NT
	300	0.250	NT	NT
	600	0.062	NT	NT
	1200	-0.052	NT	NT
10% DMSO in saline	-	0.880	0.941	1.069
4-NQO	-	0.508	5.143	10.126

[a] G (growth factor) = (mean A_{600} of tested sample) – (mean A_{600} of blank) / (mean A_{600} of negative control) – (mean A_{600} of blank), G > 0.5 – necessary condition for the reliability of the test results, G < 0.5 – toxicity towards the used bacterial strains; [b] U_s (β-galactosidase activity, relative units) = (mean A_{420} of tested sample) – (mean A_{420} of blank) / (mean A_{420} of negative control) – (mean A_{420} of blank); [c] I_R (induction ratio) = $1/G*U_s$, $I_R > 1.5$ – genotoxicity in a particular concentration; 4-NQO – 4-nitroquinoline *N*-oxide; NT – not tested; - – not applicable.

2.4. *In silico* metabolism prediction

Additional assays related to safety of active compounds include metabolism prediction. The MetaSite program (Cruciani et al., 2005; Boyer et al., 2009) allows *in silico* prediction of possible routes of metabolism, including skin metabolism. It is particularly important for antibacterial compounds, which are frequently applied topically. The performed *in silico* prediction revealed

that the most probable sites of metabolism are methylene group of hydroxyethyl substituent at the piperazine ring together with the nitrogen atom, to which the hydroxyethyl is attached. According to performed simulations, the most probable metabolites (Scheme 2) are products of oxidation: (1) aldehyde or carboxylic acid resulting from opening of the piperazine ring, (2) amide resulting from oxidation of methylene group into carbonyl moiety and (3) *N*-oxide, which have been previously subject of our research in a group of piperazine derivatives (Żesławska et al., 2020). Another product is a result of disconnection of the hydroxyethyl substituent at the piperazine ring. Concluding the observed predictions, together with observations of data provided by the program, the xanthone moiety remains stable in the *in silico* prediction, which is also consistent with our former *in silico* and *in vitro* findings for alkoxy derivatives of xanthone with aminoalkanol substituents (Waszkielewicz et al., 2016). Moreover, the program has indicated that the hydroxyethyl substituent is oxidized into glycolic acid in the process of oxidative hydrolysis from piperazine, which may – consistently with the data on beneficial activity of α-hydroxyacids (Yu & Van Scott, 2004) – contribute to further activity after absorption and metabolism in the skin. Moreover, from the perspective of our further research objectives, it will be interesting to synthesize some of the metabolites and study their properties. Metabolites containing aldehyde group seem too reactive to plan administration in skin (potential reaction with amine groups of amino acids and resulting colouring properties). Synthesis of other metabolites or research regarding analysis of *in vivo* metabolites are interesting for our further research.

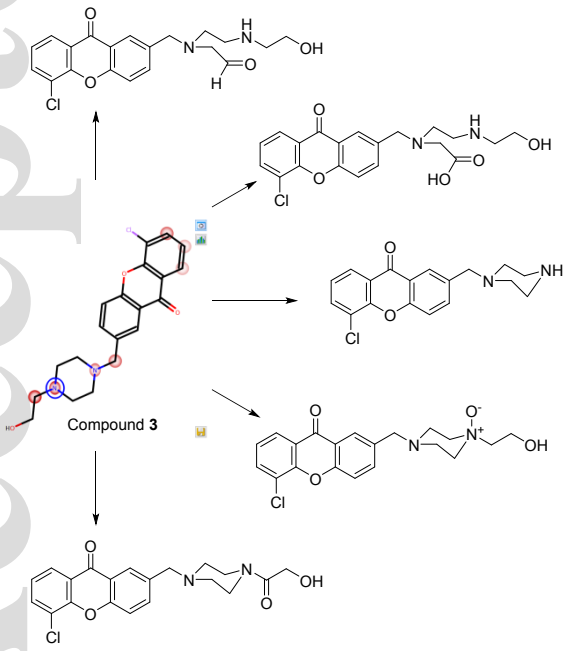

Scheme 2 The most probable sites of metabolism of Compound **3** marked as coloured rings on the structure as well as its five most probable metabolites according to *in silico* prediction of skin metabolism.

3. Conclusions

As a conclusion, this research resulted in achievement of a very potent antibacterial compound 5-chloro-2-((4-(2-hydroxyethyl)piperazin-1-yl)methyl)-9*H*-xanthen-9-one dihydrochloride (**3**), exhibiting MIC of 0.8 μg/mL against *Staphylococcus epidermidis* ATCC 12228 strain.

Another conclusion is high importance of position C2 for piperazinemethyl substituents in the xanthone moiety for the antibacterial activity when Cl is present at C5, in spite of enlargement of molecular volume of the compound compared to C4 analogs. Nevertheless, calculation of the physical-chemical properties still remains important part in chemical drug design.

The last conclusion is the safety in terms of genotoxicity of the active compound **3** at 75 μg/mL and surprisingly potential antibacterial activity against *Salmonella enterica* at higher concentrations, as well as promising *in silico* predictions of the compound's metabolism in the skin. Therefore, there exist premises for further research in this group of compounds in terms of multiple antibacterial activity.

4. Experimental protocols

4.1. Chemistry

All reagents were manufactured by Alfa Aesar (purchased from Chemat, Gdansk, Poland or Trimen Chemicals S.A., Łódź, Poland), or Sigma-Aldrich (purchased from Sigma-Aldrich, Poznan, Poland). Solvents were commercially available materials of reagent grade. Melting points (mp) were determined by means of a Büchi Melting Point M-560 apparatus (Büchi Labortechnik, Flawil, Switzerland) and were uncorrected. The purity of the obtained compounds was confirmed by LCMS at Faculty of Pharmacy, Jagiellonian University Medical College. For mass spectrometry analysis samples were prepared in acetonitrile/water (10/90 v/v) mixture. The LC/MS system consisted of a Waters Acquity UPLC, coupled to a Waters TQD mass spectrometer (electrospray ionization mode ESI-tandem quadrupole). All the analyses were carried out using an Acquity UPLC BEH C18, 1.7 lm, 2.1 x 100 mm column. A flow rate of 0.3 mL/min and a gradient of (5 – 95) % B over 10 min and then 100% B over 2 min was used. Eluent A: water / 0.1 %

HCO_2H; eluent B: acetonitrile / 0.1% HCO_2H. LC/MS data were obtained by scanning the first quadrupole in 0.5 s in a mass range from 50 to 1000 Da; eight scans were summed up to produce the final spectrum.

The ^1H NMR spectra were obtained at Faculty of Pharmacy, Jagiellonian University Medical College, using Bruker AVANCE III 600 (600.2 MHz) spectrometer (Bruker, Karlsruhe, Germany). Results are presented in the following format: chemical shift δ (ppm), multiplicity, *J* values in Hertz (Hz), number of protons, protons' position. Multiplicities are showed as the abbreviations: s (singlet), br s (broad singlet), d (doublet), br d (broad doublet), t (triplet), br t (broad triplet), m (multiplet).

In silico registration and interpretation of LCMS and NMR spectra were facilitated by ACDLabs 2019 Spectrus Processor 1.3.

Elemental analysis was performed at Faculty of Pharmacy, Jagiellonian University Medical College, with use of Elementar Analysensysteme GmbH VarioEL V2.10 20.Aug. 2001 CHNS Mode.

4.1.1. General procedure for preparation of the final compounds 1-10.

In the first step, reaction of condensation of 2,3-dichlorobenzoic acid with *p*-cresol or *o*-cresol, respectively, was performed. 23 g of metallic sodium was slowly (in small portions) dissolved in 500 mL of methanol. Next, 500 g of 2,3-dichlorobenzoic acid, 60 mL of *p*-kresol or *o*-kresol (respectively) and catalysts: 0,1 g Cu_2O and 0,3 g Cu were added. Reaction was heated on electromagnetic stirrer to 120 ^oC for 5 hours. During this time all the solvent (methanol) was distilled of. Then, 250 mL of paraffin oil was added and the mixture was stirred in temperature 180 ^oC for next 4 hours. After his time, the precipitate was filtered off, washed with toluene, than heptane and dried. The precipitate was dissolved in 20% water solution of NaOH, heated to 100 ^oC and stirred for 30 minutes. After this time undissolved precipitate was filtered off on a Büchner funnel. The filtrate was transferred to a separating funnel, benzene was added and the phases were separated. The water phase was collected, active carbon was added. After night the carbon and impurities were filtered of. Obtained filtrate was acidified with 10% HCl in order to obtain product of condensation (3-chloro-2-(2-methylphenoxy) or 3-chloro-2-(4-methylphenoxy) benzoic acid, respectively). The resulting precipitate was filtered off and dried.

The next step was cyclization. The crude product of condensation was dissolved in 500 mL of concentrated sulfuric acid (H_2SO_4 conc.), heated to 100 ^oC and stirred for 4 hours. The mixture

was then poured onto ice and filtered on a Büchner funnel. The precipitate was washed with water, transferred to a beaker and 20% NaOH was added, in order to wash away the 2,3-dichlorobenzoic acid that has not reacted. Undissolved precipitate was filtered off on a Büchner funnel and washed with water to give 5-chloro-4-methylxanthone. The product of cyclization was then recrystallized from ethanol, in order to obtain pure compound 1 or 8 respectively. These compounds were also used in the next step as a substrates for bromination.

For bromination of 5-chloro-4-methylxanthone or 5-chloro-2-methylxanthone, respectively, appropriate substrate, together with *N*-bromosuccinimide and benzoyl peroxide were dissolved in CCl_4, stirred in temperature of 100 ^oC on electromagnetic stirrer with reflux condenser and with additional light from UV-VIS lamp for 20 hours. After this time evolved succinimide was filtered off. The filtrate was placed in the refrigerator overnight. Obtained precipitate was filtered off, dried and recrystallized from toluene, to obtain 5-chloro-4-methylxanthone or 5-chloro-4-methylxanthone bromide, respectively.

0.02 mole of appropriate bromide was refluxed with 0.02 mole of appropriate *N*-substituted piperazine in toluene with presence of anhydrous K_2CO_3 at 110 °C for 72 h. Then the solvent was distilled off and the remaining solid, containing substrates and the product were boiled in water acidified with 10% HCl for acidic pH in order to dissolve KCl, K_2CO_3, unreacted amine and the product. The mixture was added carbon for binding the unreacted bromide and then filtered off. In order to achieve basic pH, 30% NaOH was added to the filtrate so that the product was precipitated and obtained in the form of base (the unreacted piperazine substrate was liquid). The mixture was left for several h and then filtered off. After drying the product was dissolved in boiling 96% ethanol and carbon was added to the solution for purification. After filtering of the solution, a few milliliters of 37% HCl_{aq} was added in order to precipitate the hydrochloride product, which was then left to cool down and the precipitate was then filtered off and recrystallized from methanol. The purity was verified by LC-MS. The structure was verified with LC-MS (mass), ^1H NMR (and ^{13}C NMR in cases of **1**-**4**, **8**) and – since protons at *N* were not visible in ^1H NMR – elemental analysis for determination if the salts were mono-, di- or trihydrochlorides.

4.1.2 Characterization of final products

*5-chloro-2-methyl-9H-xanthen-9-one (**1**)* White solid; yield = 73%; $C_{14}H_9ClO_2$; M = 244.03; mp 110-112 °C; ^{1}H NMR (600 MHz, D_2O) δ (ppm): 8.15 (dd, *J*=7.73, 1.43 Hz, 1 H, X-H8), 7.99 (s, 1H, X-H1), 7.68 (dd, *J*=7.73, 1.43 Hz, 1H, X-H6), 7.44 - 7.49 (m, 1H, X-H3), 7.38 (d, *J*=8.59 Hz, 1H, X-H4), 7.22 (t, *J*=7.73 Hz, 1H, X-H7), 2.40 (s, 3H, -CH_3); ^{13}C NMR (126 MHz, CHLOROFORM-*d*) δ ppm 176.55 (s, 1C, C=O), 154.02 (s, 1C, X-C4a), 151.74 (s, 1C, X-C4b), 136.45 (s, 1C, , X-C3), 134.78 (s, 1C, X-C6), 134.42 (s, 1C, X-C2), 126.00 (s, 1C, X-C1), 125.35 (s, 1C, X-C7), 123.65 (s, 1C, X-C8), 123.08 (s, 1C, X-C5), 122.80 (s, 1C, X-C8a), 121.00 (s, 1C, X-C8b), 118.00 (s, 1C, X-C4), 20.91 (s, 1C, -***C***H_3); LC-MS $[M + H]^+$ m/z: 245.23, 99.19%.

*5-chloro-2-(((2-hydroxyethyl)amino)methyl)-9H-xanthen-9-one hydrochloride (**2**),* Light beige solid; yield = 63%; $C_{14}H_9ClO_2$; M = 303.07; mp 281-283 °C; ^{1}H NMR (600 MHz, DMSO-d_6) δ (ppm): 9.66 (br s, 1H, NH^+), 8.36 (d, J = 2.3 Hz, 1H, X-1), 8.16–8.12 (m, 1H, X-8), 8.12–8.09 (m, 1H, X-6), 8.02–7.99 (m, 1H, X-3), 7.74 (d, J = 8.6 Hz, 1H, X-4), 7.43 (t, J = 7.7 Hz, 1H, X-7), 5.31 (br s, 1H, -OH), 4.28 (br s, 2H, -NH), 3.68 (t, J = 5.4 Hz, 2H, X-CH2-NH), 3.34 (br s, 2H, NH-CH2-CH2-OH), 2.95 (br s, 2H, NH-CH2-CH2-OH); ^{13}C NMR (126 MHz, DMSO-d_6) δ ppm 175.89 (s, 1C, C=O), 155.79 (s, 1 C, X-C4a), 151.57 (s, 1C, X-C4b), 138.39 (s, 1C, X-C2), 136.09 (s, 1C, X-C6), 129.47 (s, 1C, X-C3), 128.93 (s, 1C, X-C1), 125.62 (s, 1C, X-C7), 125.38 (s, 1C, X-C8), 123.16 (s, 1C, X-C5), 122.24 (s, 1C, X-C8a), 121.10 (s, 1C1, X-C8b), 119.12 (s, 1C, X-C4), 56.86 (s, 1C, NH-CH_2-***C***H_2-OH), 49.44 (s, 1C, X-***C***H_2-NH), 49.19 (s, 1C, NH-***C***H_2-CH_2-OH); LC-MS $[M + H]^+$ m/z: 304.18, 99.31%.

*5-Chloro-2-((4-(2-hydroxyethyl)piperazin-1-yl)methyl)-9H-xanthen-9-one dihydrochloride (**3**).* Yellow solid; yield = 92%; $C_{20}H_{23}N_2O_3Cl_3$; M = 372.12; mp 290-292 °C; el.an. $^{calc}/_{anal}$: $N^{6.28}/_{6.18}$; $C^{53.89}/_{53.89}$; $H^{5.20}/_{5.21}$; ^{1}H NMR (600 MHz, D_2O) δ (ppm): 7.71 (d, *J* = 1.7, 1H, X-1), 7.64-7.60 (m, 1H, X-6), 7.45-7.41 (m, 1H, X-4), 7.33-7.29 (m, 1H, X-3), 7.09 (d, *J* = 8.6, 1H, X-8), 6.92 (t, *J* = 8.0, 1H, X-7), 4.35 (s, 2H, X-CH_2-N<), 3.86-3.81 (m, 2H, >N-CH_2-CH_2-OH), 3.64 (br s, 4H, pip), 3.56 (br s, 4H, pip), 3.37-3.33 (m, 2H, >N-C*H*$_2$-CH_2-OH). ^{13}C NMR (126 MHz, D_2O) δ (ppm): 176.8 (X-9), 155.6 (X-4'), 150.4 (X-5'), 138.4 (X-3), 136.2 (X-6), 128.9 (X-2), 124.9 (X-7), 124.8 (X-1), 124.4(X-8), 122.1 (X-5), 120.9 (X-8'), 119.8 (X-9'), 119.5(X-4), 59.2 (X-*C*H_2-N<), 58.2 (>N-*C*H_2-CH_2-OH), 54.9 (>N-CH_2-*C*H_2-OH), 48.9 (pip: N-CH_2-*C*H_2-N-), 48.1(pip: N-*C*H_2-CH_2-N-); LC-MS $[M + H]^+$ m/z: 373.23, 98.03%.

*5-chloro-2-((4-(2-(2-hydroxyethoxy)ethyl)piperazin-1-yl)methyl)-9H-xanthen-9-one dihydrochloride (**4**):* White solid; yield = 82%; $C_{22}H_{27}N_2O_4Cl_3$; M = 453,13; el.an. $^{calc}/_{anal}$:

$N^{5.72}/_{5.63}$; $C^{53.95}/_{53.74}$; $H^{5.56}/_{5.55}$; mp 270-272 °C; ^{1}H NMR (600 MHz, D_2O) δ (ppm): 7.70 (s,1H, X-1), 7.65-7.59 (m, 1H, X-8), 7.43-7.37 (m, 1H, X-3), 7.27 (d, *J* = 8.0, 1H, X-4), 7.06 (d, *J* = 8.6, 1H, X-6), 6.93-6.85 (m, 1H, X-7), 4.36 (s, 2H, X-C*H*$_2$-N<), 3.82-3.73 (m, 3H, >N-CH$_2$-C*H*$_2$-O, -OH), 3.72-3.61 (m, 6H, pip, O-C*H*$_2$-CH$_2$-OH), 3.60-3.53 (m, 6H, pip, >N-CH$_2$-C*H*$_2$-O), 3.46-3.44 ppm (m, 2H, >N-C*H*$_2$-CH$_2$-O). ^{13}C NMR (126 MHz, D_2O) δ (ppm): 176.67 (X-C9, C=O), 155.51 (X-C4a), 150.35 (X-C4b), 138.43 (X-C3), 136.22 (X-C6), 128.96 (X-C2), 124.87 (X-C7), 124.71(X-C1), 124.35 (X-C8), 122.01 (X-C5), 120.83 (X-C8a), 119.73 (X-C9a), 119.47 (X-C4), 71.85 (O-*C*H$_2$-OH), 63.51 (>N-CH$_2$-*C*H$_2$-O), 60.44 (X-*C*H$_2$-N<), 59.1 (O-*C*H$_2$-CH$_2$-OH), 48.96 (pip: N-*C*H$_2$-CH$_2$-N), 48.16 (pip: N-CH$_2$-*C*H$_2$-N); LC-MS $[M + H]^+$ m/z: 417.23, 99.36%.

*5-chloro-2-((4-phenethylpiperazin-1-yl)methyl)-9H-xanthen-9-one dihydrochloride (**5**)*. Light grey solid; yield = 78%; $C_{26}H_{27}N_2O_2Cl_3$; M = 504.11; mp 291-293 °C; el.an. $^{calc}/_{anal}$: $N^{5.54}/_{5.42}$; $C^{61.73}/_{61.67}$; $H^{5.38}/_{5.48}$;^{1}H NMR (600 MHz, acetone-d_6) δ (ppm): 8.24-8.14 (m, 2H, X-6, X-7); 7.96-7.93 (m, 1H, X-8), 7.87 (dd, *J* = 8.59, 2.29, 1H, X-3), 7.65 (d, *J* = 8.59, 1H, X-4), 7.46-7.43 (m, 1H, X-1), 7.25 - 7.19 (m, 4H, Fen-2, Fen-3, Fen-5, Fen-6), 7.15-7.12 (m, 1H, Fen-4), 3.62 (s, 2H C*H*$_2$-N<), 2.79-2.71 (m, 4H, >N-C*H*$_2$-C*H*$_2$-Fen), 2.54- 2.42 (m, 8H, pip). LC-MS $[M + H]^+$ m/z: 433.24, 100.00%.

*2-((4-(benzo[d][1,3]dioxol-5-ylmethyl)piperazin-1-yl)methyl)-5-chloro-9H-xanthen-9-one dihydrochloride (**6**)*. Light beige solid; yield = 65%; $C_{26}H_{25}N_2O_4Cl_3$; M=535.85; mp 296-298 °C; el.an. $^{calc}/_{anal}$: $N^{5.23}/_{5.13}$; $C^{58.28}/_{57.91}$; $H^{4.70}/_{4.60}$; ^{1}H NMR (600 MHz, DMSO-d_6) δ (ppm) 10.90 (br s, 1H, HCl), 8.14 – 8.04 (m, 2H, X-1, X-8), 8.01 (br d, *J* = 7.4, 1H, X-6), 7.86 – 7.73 (m, 1H, X-4), 7.67 (br d, *J* = 8.0, 1H, X-3), 7.43 (br t, *J* = 7.9, 1H, X-7), 7.23 (br s, 1H, PIPER-4), 7.00 (br s, 1H, PIPER-7), 6.92 (br d, *J* = 7.2, 1H, PIPER-6), 6.01 (br s, 2H, PIPER-2, (O-C*H*$_2$-O)), 3.66 (br s, 2H, >N-C*H*$_2$-PIP), 3.31 (s, 6H, X-C*H*$_2$-N<, N<C*H*$_2$, (piperazine)), 3.07–2.75 (m, 4H, C*H*$_2$>N (piperazine)); LC-MS [M + H]+ m/z: 463.24, 100.00%.

*5-chloro-2-((4-(pyridin-2-yl)piperazin-1-yl)methyl)-9H-xanthen-9-one trihydrochloride (**7**)*. Light beige solid; yield: 61%; $C_{23}H_{23}N_3O_2Cl_4$; M = 513.05; mp 281-283 °C; el.an. $^{calc}/_{anal}$: $N^{8.16}/_{8.22}$; $C^{53.61}/_{54.61}$; $H^{4.50}/_{4.71}$;^{1}H NMR (600 MHz, $CDCl_3$) δ (ppm): 8.27-8.22 (m, 2H, X-1, pyr-6); 8.18-8.14 (m, 1H, X-8); 7.86-7.82 (m, 1H, X-6); 7.77 (d, *J* = 8.02, 1H, X-4); 7.59 (d, *J* = 8.59, 1H, X-3); 7.48-7.41 (m, 1H, pyr-4); 7.30 (t, *J* = 7.73, 1H, X-7); 6.64-6.57 (m, 2H, pyr-3,5); 3.66 (s, 2H, 2X-CH$_2$); 3.58-3.50 (m, 4H, Pip-N1-(CH$_2$-C*H*$_2$)$_2$-N4); 2.58 (br t, *J* = 4.87, 4H, Pip-N1-(C*H*$_2$-CH$_2$)$_2$-N4). LC-MS $[M + H]^+$ m/z: 406.128, 100.00%.

4-chloro-5-methyl-9H-xanthen-9-one ***(8)*** Light yellow solid; yield: 71%; $C_{14}H_9ClO_2$; M= 244.03; mp 116.8-117.7°C ^{1}H NMR (500 MHz, DMSO-d_6) δ ppm 8.00 (dd, *J*=8.02, 1.43 Hz, 1H, X-H8), 7.90 (dd, *J*=7.73, 1.72 Hz, 1H, X-H1), 7.80 (d, *J*=1.15 Hz, 1H, X-H2), 7.57 (dd, *J*=8.73, 2.15 Hz, 1H, X-H6), 7.44 (d, *J*=8.59 Hz, 1H, X-H3), 7.34 (t, *J*=7.88 Hz, 1H, X-H7), 2.34 (s, 3H, -CH_3); ^{13}C NMR (126 MHz, DMSO-d_6) δ ppm 175.80 (s, 1C, C=O), 153.84 (s, 1C, X-C4a), 151.39 (br s, 1C, X-C4b), 137.38 (br d, *J*=3.62 Hz, 1C, X-C3), 135.64 (br s, 1C, X-C6), 134.90 (br s, 1C, X-C7), 125.69 (s, 1C, X-C4), 125.47 (s, 1C, X-C2), 124.87 (s, 1C, X-C8), 122.95 (d, *J*=3.02 Hz, 1C, X-C8a), 122.11 (s, 1C, X-C5), 120.81 (br s, 1C, X-C8b), 118.48 (br s, 1C, X-C1), 20.83 (s, 1C, -***C***H_3); LC-MS $[M + H]^+$ m/z: 245.04.128, 100.00%.

4-chloro-5-((4-(2-hydroxyethyl)piperazin-1-yl)methyl)-9H-xanthen-9-one dihydrochloride ***(9)***. White solid; yield: 76%; $C_{20}H_{23}N_2O_3Cl_3$; M=445.77; el.an. $^{calc}/_{anal}$: $N^{6.28}/_{6.22}$; $C^{53.89}/_{54.71}$; $H^{5.20}/_{5.60}$; mp 291-293 °C; ^{1}H NMR (600 MHz, D_2O) δ (ppm): 7.89 (d, *J* = 8.0, 1H, X-1), 7.81 (d, *J* = 7.4, 1H, X-8), 7.67 (d, *J* = 8.0, 1H, X-3), 7.65-7.61 (m, 1H, X-6), 7.31 (t, *J* = 7.7, 1H, X-7), 7.12 (t, *J* = 7.7, 1H, X-2), 4.45 (s, 2H, X-CH_2-N<), 3.81-3.77 (m, 2H, >N-CH_2-CH_2-OH), 3.68 -3.45 (br s, 8H, -CH2- (pip)), 3.31-3.27 (m, 2H, >N-CH_2-CH_2-OH). LC-MS $[M + H]^+$ m/z: 373.15, 99.21%.

4-chloro-5-((4-(2-(2-hydroxyethoxy)ethyl)piperazin-1-yl)methyl)-9H-xanthen-9-one dihydrochloride ***(10)***. White solid; yield = 75%; $C_{22}H_{27}N_2O_4Cl_3$; M = 489.82; mp 281-283 °C; el.an. $^{calc}/_{anal}$: $N^{5.72}/_{5.60}$; $C^{53.95}/_{54.36}$; $H^{5.56}/_{5.81}$; ^{1}H NMR (600 MHz, D_2O) δ (ppm): 7.80 (br d, *J* = 7.4, 1H, X-1), 7.78 (br d, *J* = 8.6, 1H, X-8), 7.53 (t, *J* = 7.2, 2H, X-3, X-6), 7.26 (t, *J* = 7.7, 1H, X-7), 7.02 (t, *J* = 7.7, 1H, X-2), 4.45 (s, 2H, X-CH_2-N<), 3.76–3.71 (m, 2H, -O-CH_2-CH_2-OH), 3.68–3.58 (m, 8H, CH_2- (pip)), 3.58 (br d, *J* = 4.6, 2H, >N-CH_2-CH_2-O-), 3.51–3.48 (m, 2H, -O-CH_2-CH_2-OH), 3.41–3.37 (m, 2H, >N-CH_2-CH_2-O-). LC-MS $[M + H]^+$ m/z: 417.29, 100.00%.

4.2. Microbiology

The bacteria used are *Staphylococcus epidermidis* ATCC 12228 (Winslow and Winslow) and clinical strain K/12/8915 obtained from the collection of the Department of Pharmaceutical Microbiology, Faculty of Pharmacy, Jagiellonian University Medical College. Strains were exposed to the newly synthetized compounds using dilution method in a 96-well polystyrene flat-bottomed microtiter plates. Protocols for MIC (Minimum Inhibitory Concentration) determinations were based on the EUCAST guidelines

(http://www.eucast.org/ast_of_bacteria/media_preparation/). The MIC value of the newly tested compounds was determined in CAMHB II broth (Cation-Adjusted Mueller-Hinton Broth, BD BBL™). New synthetized compounds were dissolved in DMSO (1% of the final volume, Merck) and diluted with culture broth to a concentration of 50 μg/mL. Further 1:2 serial dilutions were performed by addition of culture broth to reach concentrations ranging from 50 to 0.1 μg/mL. In the assay, control of the Cation-Adjusted Mueller-Hinton Broth (CAMHB II) with the new compounds was also performed and no increase in the absorbance value was observed compared to the control of the broth itself. The reference chemotherapeutic agents: linezolid, ciprofloxacin, sulfamethoxazole in combination with trimethoprim were purchased from Merck and dissolved in DMSO. The study carried out quality control of sensitivity determination for linezolid, ciprofloxacin and trimethoprim / sulfometaxazole against the *Staphylococcus aureus* ATCC 29213 control strain (internal quality control EUCAST). The plates were incubated at 37 °C for 18 to 20 h with shaking and the optical density was read in a microtiter plate reader Sunrise™ (Tecan, Switzerland) at 600 nm. MICs for antimicrobial compound-treated cultures were calculated as the lowest concentration of compound/drug at which growth was not apparent, as measured by optical density at 600 nm. All experiments were performed at least in triplicate and the average MIC was listed as the MIC in data Table 1.

4.3 Genotoxicity

Potential genotoxicity was tested with a use of commercially available UMU-Chromotest kit (EBPI, environmental bio-detection products inc., Canada, http://www.ebpi.ca, accessed 06 February 2020; ISO 13829: Water quality-determination of the genotoxicity of water and waste water using the umu-test, 2003-03-15). All reagents and solvents were provided with the kit. Photometer Eppendorf BioPhotometer plus LabtechLT-4000 Microplate Reader were used for absorbance measurements. Experiments were carried out according to a procedure attached to the kit (UMU-Chromotest Procedure, Version 6.6).

Briefly, one day before the experiment dried bacteria (engineered *Salmonella typhimurium* strain) were rehydrated and incubated overnight at 37 °C. After 18 h the previously prepared bacterial culture showed OD_{600} reading approximately 0.5. After dilution by half with a growth medium, it was placed in an incubator for additional 1.5 h (37 °C). In the meantime, a test microplate A has been prepared. Stock solutions of tested compounds were prepared in 10%

DMSO in saline. Subsequently, they were pipetted on a microplate and diluted with distilled water in order to obtain final concentrations (each tested in triplicate). 10% DMSO in saline served for a solvent control, water for a negative control, 4-NQO solution (included in the kit) for a positive control, while appropriate amounts of distilled water and growth media served for blank. Finally, each well was supplemented with 20 µL of growth media enriched with glucose. After 1.5 h incubation, bacterial culture were pipetted to all wells (excluding blank) and the microplate A was incubated at 37 °C for 2 h. Then, 30 µL from each well of microplate A was pipetted into the corresponding well of microplate B and diluted tenfold with growth media enriched with glucose. Subsequently, microplate B was incubated at 37 °C for 2 h and after that time absorbance at 600 nm was measured in order to calculate growth factor (G = mean A_{600} of tested sample – mean A_{600} of blank / mean A_{600} of negative control – mean A_{600} of blank, final results considered valid if G>0.5). Then, microplate C was prepared by adding to each well: 270 µL of B-buffer, 30 µL from a corresponding microplate B well and 30 µL of *o*-nitrophenyl-ß-galactoside solution in phosphate buffer. Plate C was immediately placed in an incubator at 37 ℃ for 30 min, after which time yellow colour developed in a positive control wells and 120 µL of Stop Solution was added to all wells of microplate C. The absorption of the solution in each well was measured at 420 nm. β-galactosidase activity (U_s = mean A_{420} of tested sample – mean A_{420} of blank / mean A_{420} of negative control – mean A_{420} of blank) and induction ratio ($I_R = 1/G*U_s$) were calculated for samples with G > 0.5. If I_R > 1.5, a compound was considered genotoxic in a particular concentration.

4.4. Metabolism prediction

The prediction of metabolism was performed with use of MetaSite 6.0.1 x64 (Molecular Discovery), version built on March 20th 2018.

Conflicts of interest

There are no conflicts to declare.

The data that supports the findings of this study are available in the supplementary material of this article.

Bibliography

Baym, M., Stone, L. K. & Kishony, R. (2016) Multidrug evolutionary strategies to reverse antibiotic resistance. *Science*, 351, aad3292. https://doi.org/10.1126/science.aad3292

Bizzarro, M. J., Shabanova, V., Baltimore, R. S., Dembry, L.-M., Ehrenkranz, R. A. & Gallagher, P. G. (2015). Neonatal Sepsis 2004-2013: The Rise and Fall of Coagulase-Negative Staphylococci, *The Journal of Pediatrics*, 166(5), 1193-1199. https://doi.org/10.1016/j.jpeds.2015.02.009

Boyer, D., Bauman, J. N., Walker, D. P., Kapinos, B., Karki, K. & Kalgutkar, A. S. (2009). Utility of MetaSite in Improving Metabolic Stability of the Neutral\nIndomethacin Amide Derivative and Selective Cyclooxygenase-2\nInhibitor 2-(1-(4-Chlorobenzoyl)-5-Methoxy-2-Methyl-1H-Indol-3-\nyl)-N-Phenethyl-Acetamide, *Drug Metabolism and Disposition*, 37(5), 999–1008. https://doi.org/10.1124/dmd.108.026112.be

Brzychczy-Wloch, M., Borszewska-Kornacka, M., Gulczynska, E., Wojkowska-Mach, J., Sulik, M., Grzebyk, M., Luchter, M., Heczko, P. B. & Bulanda, M. (2013) Prevalence of Antibiotic Resistance in Multi-Drug Resistant Coagulase-Negative Staphylococci Isolated from Invasive Infection in Very Low Birth Weight Neonates in Two Polish NICUs, *Annals of Clinical Microbiology and Antimicrobials,* 12(1), 1–7. https://doi.org/10.1186/1476-0711-12-41

Büttner, H., Mack, D. & Rohde, H. (2015) Structural Basis of Staphylococcus Epidermidis Biofilm Formation: Mechanisms and Molecular Interactions, *Frontiers in Cellular and Infection Microbiology*, *5*(February), 1–15. https://doi.org/10.3389/fcimb.2015.00014

Cheung, G. Y. C. & Otto, M. (2010) Understanding the Significance of Staphylococcus Epidermidis Bacteremia in Babies and Children, *Current Opinion in Infectious Diseases*, 23(3), 208–21. https://doi.org/10.1126/scisignal.2001449.Engineering

Cruciani, G., Carosati, E., De Boeck, B., Ethirajulu, K., Mackie, C., Howe, T. & Vianello, R.

(2005) MetaSite: Understanding Metabolism in Human Cytochromes from the Perspective of the Chemist, *Journal of Medicinal Chemistry,* 48(22), 6970–6979. https://doi.org/10.1021/jm050529c

Dersch, P., Khan M. A., Mühlen S. & Görke, B. (2017) Roles of Regulatory RNAs for Antibiotic Resistance in Bacteria and Their Potential Value as Novel Drug Targets. *Frontiers in Microbiology*, 8, 803. https://doi.org/10.3389/fmicb.2017.00803

Dharmaratne, H. R. W., Sakagami, Y., Piyasena, K. G. P., Thevanesam, V. (2013) Antibacterial Activity of Xanthones from Garcinia Mangostana (L.) and Their Structure-Activity Relationship Studies, *Natural Product Research,* 27(10), 938–941. https://doi.org/10.1080/14786419.2012.678348

Eckstein, M. & Marona, H. (1980) Preparation and Properties of Some 2-Mercaptomethylxanthones, *Polish Journal of Chemistry,* 54, 1281-1285.

Eftekhar, F., & Speert, D. P. (2009) Biofilm Formation by Persistent and Non-Persistent Isolates of Staphylococcus Epidermidis from a Neonatal Intensive Care Unit, *Journal of Hospital Infection,* 71(2), 112–116. https://doi.org/10.1016/j.jhin.2008.09.008

Fell, D. B., Hawken, S., Wong, C. A., Wilson, L. A., Murphy, M. S. Q., Chakraborty, P., Lacaze-Masmonteil, T., Potter, B. K. & Wilson, K. (2017) Using Newborn Screening Analytes to Identify Cases of Neonatal Sepsis, *Scientific Reports,* 7(1), 1–10. https://doi.org/10.1038/s41598-017-18371-1

Fitzpatrick, F., Humphreys & H., O'Gara, J. P. (2005) The Genetics of Staphylococcal Biofilm Formation - Will a Greater Understanding of Pathogenesis Lead to Better Management of Device-Related Infection?, *Clinical Microbiology and Infection*, 11(12), 967–973. https://doi.org/10.1111/j.1469-0691.2005.01274.x

Fukai, T., Oku, Y., Hou, A-J., Yonekawa, M. & Terada, S. (2005) Antimicrobial Activity of Isoprenoid-Substituted Xanthones from Cudrania Cochinchinensis against Vancomycin-Resistant Enterococci, *Phytomedicine,* 12(6–7), 510–513. https://doi.org/10.1016/j.phymed.2004.03.010

Jung, H-A., Su, B-N., Keller, W. J., Mehta, R. G. & Kinghorn, A. D. (2006) Antioxidant Xanthones from the Pericarp of Garcinia Mangostana (Mangosteen), *Journal of*

Agricultural and Food Chemistry, 54, 2077–2082. https://doi.org/10.1021/jf052649z

Klesiewicz, K., Karczewska, E., Budak, A., Marona, H. & Szkaradek, N. (2016) Anti-Helicobacter Pylori Activity of Some Newly Synthesized Derivatives of Xanthone, *The Journal of Antibiotics (Tokyo),* 69(11), 825–834. https://doi.org/doi: 10.1038/ja.2016.36

Klesiewicz, K., Żelaszczyk, D., Trojanowska, D., Bogusz, B., Małek, M., Waszkielewicz, A., Szkaradek, N., Karczewska, E., Marona, H. & Budak, A. (2018) Preliminary Antifungal Activity Assay of Selected Chlorine-Containing Derivatives of Xanthone and Phenoxyethyl Amines, *Chemical Bioligy Drug Design,* 92(5), 1867–1875. https://doi.org/10.1111/cbdd.13356

Koh, J.-J., Qiu, S., Zou, H., Lakshminarayanan, R., Li, J., Zhou, X., Tang, C., Saraswathi, P., Verma, C., Tan, D. T. H., Tan, A. L., Liu, S. & Beuerman, R. W. (2013) Rapid bactericidal action of alpha-mangostin against MRSA as an outcome of membrane targeting. *Biochimica et Biophysica Acta (BBA) – Biomembranes*, 1828, 834-844. https://doi.org/10.1016/j.bbamem.2012.09.004

Monserrat-Martinez, A., Gambin, Y. & Sierecki, E. (2019) Thinking Outside the Bug: Molecular Targets and Strategies to Overcome Antibiotic Resistance. *International Journal of Molecular Sciences*, 20, 1255. http://dx.doi.org/10.3390/ijms20061255

Namvar, A. E., Bastarahang, S., Abbasi, N., Ghehi, G. S., Farhadbakhtiarian, S., Arezi, P., Hosseini, M., Baravati, S. Z., Jokar, Z. & Chermahin, S. G. (2014) Clinical Characteristics of Staphylococcus Epidermidis: A Systematic Review, *GMS Hygiene and Infection Control,* 9(3), 1–10. https://doi.org/10.3205/dgkh000243

Nash, C., Chu, A., Bhatti, M., Alexander, K., Schreiber, M. & Hageman, J. R. (2013) Coagulase Negative Staphylococci in the Neonatal Intensive Care Unit: Are We Any Smarter?, *Neoreviews,* 14(6), 284-294. https://doi.org/10.1542/neo.14-6-e284

Perdih, A., Hrast, M., Barreteau, H., Gobec, S., Wolber, G. & Solmajer, T. (2014) Inhibitor design strategy based on an enzyme structural flexibility: a case of bacterial MurD ligase. *Journal of Chemical Information and Modeling*, 54, 1451−1466. http://dx.doi.org/10.1021/ci500104m

Perdih, A., Hrast, M., Pureber, K., Barrereau, H., Grdadolnik, S. G., Kocjan, D., Gobec, S.,

Solmajer, T. & Wolber, G. (2015) Furan-based benzene mono- and dicarboxylic acid derivatives as multiple inhibitors of the bacterial Mur ligases (MurC-MurF): experimental and computational characterization. *Journal of Computer-Aided Molecular Design*, 29, 541–560. http://dx.doi.org/10.1007/s10822-015-9843-6

Pinto, M. M. M., Sousa, M. E. & Nascimento, M. S. J. (2005) Xanthone Derivatives: New Insights in Biological Activities, *Current Medicinal Chemistry,* 12(21), 2517–2538. https://doi.org/10.2174/092986705774370691

Reifferscheid, G., Heil, J., Oda, Y. & Zahn, R. K. A. (1991) Microplate Version of the SOS/Umu-Test for Rapid Detection of Genotoxins and Genotoxic Potentials of Environmental Samples, *Mutation Research/Environmental Mutagenesis and Related Subjects,* 253(3), 215–222. https://doi.org/10.1016/0165-1161(91)90134-T

Rewcastle, G. W., Atwell, G. J., Baguley, B. C., Calveley, S. B. & Denny, W. A. (1989) Potential Antitumor Agents . 58 . Synthesis and Structure-Activity Relationships of Substituted Xanthenone-4-Acetic Acids Active against the Colon 38 Tumor in Vivo, *Journal of Medicinal Chemistry,* 1989, 32, 793–799. https://doi.org/10.1021/jm00124a012

Riduan, S. N., Armugam A., & Zhang, Y. (2020) Antibiotic resistance mitigation: the development of alternative general strategies. *Journal of Materials Chemistry B*, advance article. https://doi.org/10.1039/D0TB01241F

Sakagami, Y., Iinuma, M., Piyasena, K. G. N. P. & Dharmaratne, H. R. W. (2005) Antibacterial activity of α-mangostin against vancomycin resistant Enterococci (VRE) and synergism with antibiotics. *Phytomedicine*, 12, 203-208. https://doi.org/10.1016/j.phymed.2003.09.012

Singh, R., Ray, P., Das, A. & Sharma M. (2010) Penetration of antibiotics through Staphylococcus aureus and Staphylococcus epidermidis biofilms. *Journal of Antimicrobial Chemotherapy*, 65, 1955–1958. https://doi.org/10.1093/jac/dkq257

Sivaranjani, M., Leskinen, K., Aravindraja, C., Saavalainen, P., Pandian, S. K., Skurnik, M. & Ravi, A. V. (2019) Deciphering the antibacterial mode of action of α-mangostin on Staphylococcus epidermidis RP62A through an integrated transcriptomic and proteomic approach, *Frontiers in Microbiology*, 10, 160. https://doi.org/10.3389/fmicb.2019.00150

Sivaranjani, M., Prakash, M., Gowrishankar, S., Rathna, J., Pandian, S. K. & Ravi, A. V. (2017) In

vitro activity of alpha-mangostin in killing and eradicating Staphylococcus epidermidis RP62A biofilms. *Applied Microbiology and Biotechnology*, 101, 3349-3359. https://doi.org/10.1007/s00253-017-8231-7

Szkaradek, N., Gunia, A., Waszkielewicz, A. M., Antkiewicz-Michaluk, L., Cegła, M., Szneler, E. & Marona, H. (2013) Anticonvulsant Evaluation of Aminoalkanol Derivatives of 2- and 4-Methylxanthone, *Bioorganic & Medicinal Chemistry,* 21(5), 1190–1198. https://doi.org/10.1016/j.bmc.2012.12.051

Szkaradek, N., Sypniewski, D., Waszkielewicz, A. M., Gunia-Krzyżak, A., Galilejczyk, A., Gałka, S., Marona, H. & Bednarek, I. (2016) Synthesis and in Vitro Evaluation of Anticancer Potential of New Aminoalkanol Derivatives of Xanthone. *Anti-Cancer Agents in Medicinal Chemistry,* 16(12), 1587–1604. https://doi.org/10.2174/1871520616666160404110323

Wadapurkar, R. M., Shilpam, D., Kumar, A., Katti, S. & Sulochana, M. B. (2018) Informatics in Medicine Unlocked In Silico Drug Design for Staphylococcus Aureus and Development of Host-Pathogen Interaction Network, *Informatics in Medicine Unlocked*, 10(November 2017), 58–70. https://doi.org/10.1016/j.imu.2017.11.002

Waszkielewicz, A. M., Gunia, A., Szkaradek, N., Pytka, K., Siwek, A., Satała, G., Bojarski, A. J. J., Szneler, E. & Marona, H. (2013) Synthesis and Evaluation of Pharmacological Properties of Some New Xanthone Derivatives with Piperazine Moiety, *Bioorganic and Medicinal Chemistry Letters,* 23(15), 4419–4423. https://doi.org/10.1016/j.bmcl.2013.05.062

Waszkielewicz, A., Słoczyńska, K., Pękala, E., Żmudzki, P., Siwek, A., Gryboś, A. & Marona, H. (2016) Design, Synthesis and Anticonvulsant Activity of Some Derivatives of Xanthone with Aminoalkanol Moieties, *Chemical Biology Drug Design,* 89(3):339-352. https://doi.org/10.1111/cbdd.12842

Wojtyczka, R. D., Orlewska, K., Kępa, M., Idzik, D., Dziedzic, A., Mularz, T., Krawczyk, M., Miklasińska, M. & Wąsik, T. J. (2014) Biofilm Formation and Antimicrobial Susceptibility of Staphylococcus Epidermidis Strains from a Hospital Environment, *International Journal of Environmental Research and Public Health,*11(5), 4619–4633. https://doi.org/10.3390/ijerph110504619

Wright, G. D. (2016) Antibiotic Adjuvants: Rescuing Antibiotics from Resistance. *Trends in Microbiolgy*, 24, 862-871. https://doi.org/10.1016/j.tim.2016.06.009

Yu, R. J. & Van Scott, E. J. (2004) Alpha-Hydroxyacids and Carboxylic Acids, *Journal of Cosmetic Dermatology,* 3(2), 76–87. https://doi.org/10.1111/j.1473-2130.2004.00059.x

Zea-Vera, A. & Ochoa, T. J. (2015) Challenges in the Diagnosis and Management of Neonatal Sepsis, *Journal of Tropical Pediatrics,* 61(1), 1–13. https://doi.org/10.1093/tropej/fmu079

Żesławska, E., Kalinowska-Tluścik, J., Nitek, W., Marona, H. & Waszkielewicz, A. M. (2020) Influence of the Position of the Methyl Substituent and N-Oxide Formation on the Geometry and Intermolecular Interactions of 1-(Phenoxyethyl)Piperidin-4-Ol Derivatives, *Acta Crystallographica Section C: Structural Chemistry,* 76, 30–36. https://doi.org/10.1107/S2053229619015948